19th WORLD CONFERENCE OF THE ASSOCIATED RESEARCH CENTRES FOR THE URBAN UNDERGROUND SPACE
Belgrade, Serbia, November 4-7, 2025.

ACUUS BELGRADE 2025

Paper No: 2.18.120
DOI: 10.46793/ACUUS2025.2.18.120

GEOPHYSICAL IMAGING OF STOCKHOLM'S SUBSURFACE AT A MUNICIPAL SCALE— IMPLICATION FOR USE AND PLANNING OF ITS UNDERGROUND URBAN SPACE

Emmanuel Alofe[1], Mehrdad Bastani[2], Ari Tryggvason[3]

Abstract: The absence of the underground space and its usage in the current Stockholm city plan raises concerns about the urban underground space planning culture of Sweden. This issue becomes even more alarming because it is unclear, both in the literature and among practitioners, whether a map of Stockholm's subsurface exists at a municipal or district scale for planning purposes, despite the extensive use of the subsurface. Therefore, we processed airborne geophysical datasets, namely magnetic and very-low-frequency (VLF) electromagnetic, acquired over Stockholm municipality, to produce municipal-wide geophysical signature maps of the underground infrastructures in Stockholm. Stockholm's underground metro, a significant infrastructure across the city, served as a guide for the geophysical imaging, which included other underground infrastructures with similar geophysical signatures. Two maps were produced: the VLF electrical current density map, which was derived using a transformation from its raw data; and the magnetic anomaly map, which shows the residual between measured and upward continued (UC) fields. Our results show that Stockholm's central area, known as the *innerstaden* in Swedish, has a significantly higher infrastructure density than other areas, necessitating a rethink for further underground development in this area. We also find geophysical signatures, typical of major infrastructures, beneath the development focus areas proposed in the city plan outside the *innerstaden* area, which should be incorporated into the developments in these areas. Although our results are presented as 2D maps and are thus limited in the vertical dimension, the transformation algorithms and filters applied during processing were in 3D. Inspite of the results' dimensionality, they provide preliminary insights into the subsurface of Stockholm municipality at a resolution that may be suitable for strategic planning decision at a municipal scale. These results could be further developed into 3D models for a more holistic municipal-scale planning of Stockholm's underground space.

Keywords: magnetics, VLF, underground, Stockholm, planning

1. INTRODUCTION

The current Stockholm city plan—"Vision 2040 – a Stockholm for everyone." (Stockholms stad, 2018)—has no mention of the underground space nor its usage. This lack of planning for Stockholm's underground space (SUS) is alarming given the city's historic use of its subsurface (BeFo, 2018; Tengborg and Sturk, 2016). The first-come, first-served underground development approach in Sweden is well-known, both in the literature (BeFo, 2020; Bobylev, 2009; Clarke, 2000; Kuchler et al., 2024; Tengborg and Sturk, 2016; Volchko et al., 2020) and among practitioners. Conclusively, these studies have shown an urgent need for a shift towards sustainable practices, particularly if Sweden is to fulfill Goal 11 of the UN's Sustainable Development Goals (SDGs).

Several issues have been identified in the legislation and policies surrounding the planning of the Swedish underground in some of the aforementioned studies, and solutions have been proposed. However, to the best of our knowledge, there has been no published research on providing images of the underground space for planning purposes in Sweden. Meanwhile, it remains a mystery, even to practitioners, whether a 3D or even 2D map of SUS—e.g., for allocating space to new underground infrastructures—exists at a municipal or district-area scale.

[1]Mr. Alofe Emmanuel, MSc. Georesource Exploration (SINReM), doctoral researcher at the department of earth sciences, Uppsala University, Sweden, emmanuel.alofe@geo.uu.se.
[2]Dr. Bastani Mehrdad, PhD Geophysics, a senior geophysicist at the Swedish Geological Agency (SGU), Sweden, mehrdad.bastani@sgu.se.
[3]Dr. Tryggvason Ari, PhD Geophysics, associate professor at the department of earth sciences, Uppsala University, Sweden, ari.tryggvason@geo.uu.se.

Perhaps the mystery or non-existence of such information contributes to why Stockholm's underground planning (SUP) continues to receive scholarly attention without tangible action. Moreover, the invisibility of underground space has been identified as a unique challenge for urban planners and designers, a challenge that imaging capabilities used in geoscience may help solve (Admiraal and Cornaro, 2016).

The geodata national archive at *Sveriges geologiska undersökning* (SGU)—which translates to Swedish Geological Agency in English—holds nationwide geophysical measurements acquired over time at different precisions and resolutions. Airborne magnetic and very low-frequency (VLF) electromagnetic data are examples of datasets from the archive that were considered for imaging subsurface infrastructures, particularly because of their suitable sampling density. It is elementary knowledge in geophysics that air-filled or reinforced cavities in poorly magnetic or resistive bedrock exhibit a significant susceptibility and conductivity contrast, and thus are well-delineated on magnetic and VLF-derived electrical current density maps. However, VLF data, due to its narrow frequency band, have better resolution in the horizontal direction than in the vertical direction (Beamish, 1994; Pedersen et al., 1994). In practice, VLF data have been proven suitable for 2D mapping of conductive and resistive zones in the upper few hundred to tens of meters of the crust (Paal, 1965; Pedersen et al., 2009). Similarly, magnetic methods have also been effective in near-surface investigations. In fact, visual inspection of raw magnetic data, depending on its quality, is often sufficient to reveal subsurface structures (Hansen et al., 2005; Nabighian et al., 2005).

Therefore, our study aims to provide municipal-scale 2D magnetic signatures and electrical current density maps of Stockholm's underground space, which primarily consists of the Stockholm metro (subsequently referred to in its Swedish translation, *tunnelbana*) and similar structures, derived from regional airborne magnetic and VLF datasets. The objectives are to infer anthropogenic substructures from signatures observed on the two maps and analyze them in relation to the Stockholm city plan's development focus areas (DFAs), with the hope that these maps would help guide planning decisions at early developmental stages.

2. MATERIAL AND METHODS

This study's airborne magnetic and VLF data were jointly acquired in 1995 using a fixed-wing aircraft flown with 200 m line spacing at 60 m height. There are 128 lines within the study area, and measurements were taken at a frequency of 4 Hz along these lines. Most major underground infrastructures in Stockholm predate the acquisition of data.

2.1. Magnetic data

Firstly, the geomagnetic influence was removed, and the resulting magnetic anomaly data were interpolated onto a 50 m rectangular grid covering a total area of 26 x 24 km. Within this grid is a buffer zone around the administrative boundary of Stockholm municipality, which was necessary to avoid edge effects from Fourier-based filters (e.g., upward continuation) applied at a later stage. Interpolation within the grid was done using a multi-trend algorithm developed by Naprstek and Smith (2019), which is particularly suited for interpolating and enhancing thin, linear features at varying angles to the flight direction. As seen in Figure 1a, the main target, the *tunnelbana*, has lines at horizontally varying angles to the North-South flight direction.

Reduction-to-pole (RTP) was the next step in the magnetic data processing. RTP is essential for removing data dependence on the angle of geomagnetic inclination by recomputing the induced magnetic field of the sources as if they lie parallel to the magnetic pole. The structural information of the sources is not lost despite the recomputation of the RTP process (Rajagopalan, 2003).

Regional-residual magnetic fields separation was achieved through upward continuation (UC)—by removing magnetic fields that were continued upwards to 10, 30, and 60 m heights from the magnetic data, respectively. The UC of a magnetic field to a height h above a measurement plane is a mathematical technique that maps the magnetic sources from a depth of h/2 below the plane downwards (Jacobsen, 1987). This means that UC is essentially a low-pass filter that enhances the signal from magnetic sources at a specific depth and below, while attenuating those above it. It then follows that airborne magnetic data obtained at 60 m height will be theoretically equivalent to ground survey data continued upwards to 60 m. Therefore, by applying the UC filters as previously described, each residual field would contain enhanced signals from magnetic sources at 30 m depth downwards. Subsequently, we refer to the fields as the UC-separated residual fields, and in cases where specificity is required, as UCx residual field, where x is the appropriate continuation height.

As of the data acquisition date, only one metro station of the *tunnelbana* was at 35 m depth, all other subsurface stations were at an average depth of 20 m and had connections to the surface stations. Given the data flight height, it meant that the magnetic signatures of the stations would form part of the shallower high-frequency components of the UC-separated residual fields. The 2D power spectra (Spector and Grant, 1970) of each UC-separated residual fields were analyzed to choose the best, from which the depth to magnetic sources was estimated (Equation 1). In this case, the best meant the residual field that had signatures whose form is best correlated to the infrastructural layout of the *tunnelbana*. A high-pass filter with a moderate taper was applied to the chosen UC-separated residual field for enhancement of constituent wavelengths less than 1 km. The high-pass filter parameters used gave the most correlated signal of the trace target after several attempts. The analytic signal amplitude of the filtered residual field was then computed using the 3D analytic signal derivatives in Equation 2, as described by Roest et al. (1992). These authors had successfully shown that the analytic signal amplitude exhibits maxima over magnetization contrasts, thereby properly delineating magnetic sources.

$$D = -\frac{1}{4\pi} slope\ segment \xrightarrow{yields} -\frac{1}{4\pi}\left(\frac{e_2 - e_1}{k_2 - k_1} \right) \tag{1}$$

where *D* is the depth to the top of the magnetic source ensemble corresponding to each slope segment on a power spectrum in km, *e* is the log of the power amplitude, and *k* is the wavenumber in cycle/km.

$$|AS(x,y)| = \sqrt{\left(\frac{\partial M}{\partial x}\right)^2 + \left(\frac{\partial M}{\partial y}\right)^2 + \left(\frac{\partial M}{\partial z}\right)^2} \tag{2}$$

where |*AS*| is the analytic signal amplitude in nT/m; *M* is the magnetic field in nT; and *x*, *y*, and *z* are the cartesian coordinate system axes, respectively.

2.2. VLF data

The tensor tipper, relating the vertical and the two horizontal magnetic field components of the two transmitters used in the data acquisition was calculated using all the signals within a closely spaced frequency band. Estimation of the tensor tipper from multiple transmitters is well described by Pedersen et al. (1994) and is preferred because it eliminates the direction bias that would be introduced by estimating the tipper from a single transmitter. Therefore, the tensor tipper, as calculated, depends only on the subsurface conductivity structures (Pedersen et al., 2009; Pedersen and Oskooi, 2004). Pedersen and Oskooi (2004) also proved that the possible frequency dependence of tensor tipper, cautioned by Pedersen et al. (1994: 865), was not an issue in a narrow frequency band, such as in the data acquisition (15 – 30 kHz). The tensor tipper was further transformed to an apparent electrical current density map using the Becken and Pedersen (2003) transformation algorithm. The apparent current density map contained the electrical conductivity distribution of the subsurface conductors, a significant part of which is the *tunnelbana*.

3. RESULTS

The evolution of the magnetic data processing steps, from residual separation through filtering to power spectrum analysis, is presented in Figure 1. The UC10 residual field was reduced by a factor of 10 from the measured signal amplitude (cf. Figures 1b and 1c labels). This is also true for the filtered UC10 residual field (Figure 1d). However, targeted signals were still visible on the residual. Persistent regional features were further attenuated using a high-pass filter (Figure 1d).

The 2D power spectra of the residual and measured fields exhibit a two-segment slope, differing only in the second segment (Figure 1e). The highest power spectrum belonged to the UC10 residual field, but was slightly lower when compared to its filtered spectrum (Figure 1f). The labels on the power spectra are the calculated depth to the top of magnetic source ensembles for each slope segment using Equation 1.

The overlay of the *tunnelbana* layout on the analytic signal amplitude of the UC10 residual field and the apparent electrical current density are shown in Figures 2a and b, respectively. In both cases, a distinct high-magnitude signal is present along the length of the overlaid layout. The signal is evident along the entire length of the layout in some places (e.g., the green line section from *Hässelby-Vällingby* to *Enskede-Årsta-Vantör* district areas in Figure 2a and b) and partially in others. Whereas, the current density signal was visible along some sections of the layout in Figure 2a (e.g., the green line section within the *Skarpnäck* district area and the red line section within the *Skärholmen* district area), where the magnetic signal was absent.

Some signatures are not associated with the *tunnelbana* layout, e.g., around the airport located east of *Bromma*. Within the central city area—*Södermalm, Norrmalm, Kungsholmen, and Östermalm*—of Stockholm, there is a higher magnetic signature density than in the other city areas. We refer to this observation as a density bias. A similar density bias can also be observed within Farsta compared to the neighboring district areas of *Skarpnäck* and *Enskede-Årsta-Vantör* (Figure 2a). In both cases, the density biases are better observed on the magnetic analytic signal maps than on the current density maps. Figures 2c and 2d show the magnetic and apparent current density maps in relation to Stockholm's DFAs, respectively. A selection of major ongoing development projects within Stockholm was also included. Specifics of the development areas and projects gleaned from official sources (Stockholms stad, n.d., 2018; Trafikverket, 2024) are itemised in Figure 2e. Our results indicate that all of the highlighted development areas have notable magnetic signatures.

4. DISCUSSION

4.1. Geophysical imaging

According to Spector and Grant (1970), each slope segment on an average power spectrum of potential field data indicates an independent ensemble of geometrical magnetic bodies that can be characterized by a joint frequency distribution of a set of attributes. One such attribute is the depth of occurrence of the ensemble, which can be estimated from Equation 1. However, there is a condition that applies: all the magnetic bodies must be magnetized parallel to the geomagnetic vector and measured close to the north magnetic pole (Spector and Grant, 1970: 295). This requirement necessitated the reduction of the magnetic data to the magnetic north pole before the power spectrum analysis. Accordingly, all the power spectra in Figures 1e and f suggest the presence of two independent ensembles of magnetic sources. Based on depth of occurrence (2 km) and longer wavelength, the first ensemble from the left is clearly of regional geologic origin, while the other has a mix of local geologic and anthropogenic origins.

The origin of the magnetic sources becomes visually evident on the UC10 residual map (cf. Figure 1b and c). The term "residual" as used here means the magnetic field from predominantly anthropogenic magnetic sources. These residual fields exhibit similar high-frequency characteristics to the full magnetic anomaly fields shown in Figure 1e. Thus, in separating the residual fields, we used a numerically stable filter, such as the UC filter, that retains a physical meaning in the spatial domain (Jacobsen, 1987). This means that the UC30 residual field could be said to contain enhanced magnetic fields from sources between 30 and 45 m depth. This is reasonably close to the approximately 47 m depth to the top of the shallower magnetic source ensemble estimated from the statistical method of Spector and Grant (1970). However, the UC10 residual field, corresponding to 30 – 35 m depth, had a better power spectrum (Figure 1e) and is the closest to the average depth of the trace target, the *tunnelbana*. Therefore, we chose that as the best in this case. Further attenuation of persistent regional features (e.g., the fold shown in Figure 1c) using a high-pass filter enhanced the UC10 residual field, as illustrated in Figures 1d and f.

The regional-residual separation reduced the UC10 residual signal, making it difficult to delineate the outlines of the magnetic sources. The computation of the analytic signal amplitude of its filtered field revealed a high-amplitude outline that aligned with the sections of the *tunnelbana* layout that existed before the data acquisition (Figure 2a)—note the absence along ongoing sections. Computation of the analytic signal amplitude is a widely used derivative-based approach for edge delineation of magnetic structures. It maximizes over the edges of these structures (Nabighian, 1984; Roest et al., 1992). Further indications of the *tunnelbana* can also be seen in the apparent electrical current density map derived from the VLF data (Figure 2b). The correlation between the layout of the *tunnelbana* and the high-amplitude signals on both the magnetic analytic signal amplitude and electrical current density maps provides strong geophysical evidence that these signals indeed originate from the *tunnelbana*.

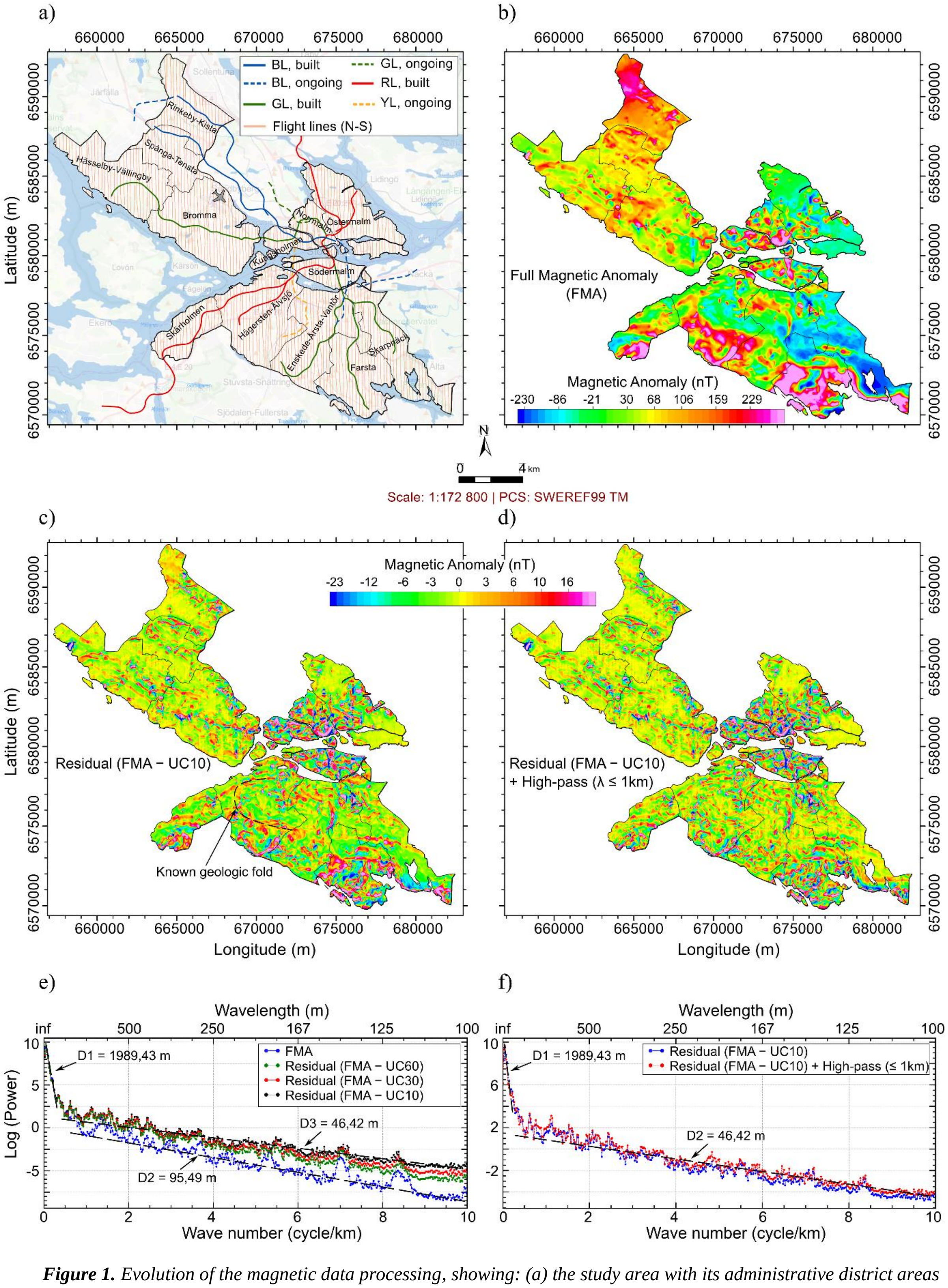

Figure 1. *Evolution of the magnetic data processing, showing: (a) the study area with its administrative district areas and an overlain layout of the targeted Stockholm's underground metro; (b) the measured magnetic anomaly field; (c) the residual magnetic anomaly field after removing (b) upward continued to 10 m from (b); (d) the high-pass filtered version of (c); (e) a comparison of the power spectra of (b) with (c) and its variants; and (f) a similar comparison between the power spectra of (c) and (d). Note how (b) had the highest power spectrum in (e), and how the effect of the filter further enhanced the signal power in (f) while attenuating the regional fold labeled in (c). D1-3 are the depths of magnetic source ensembles represented by the slope segments of the power spectra according to Spector and Grant (1970).*

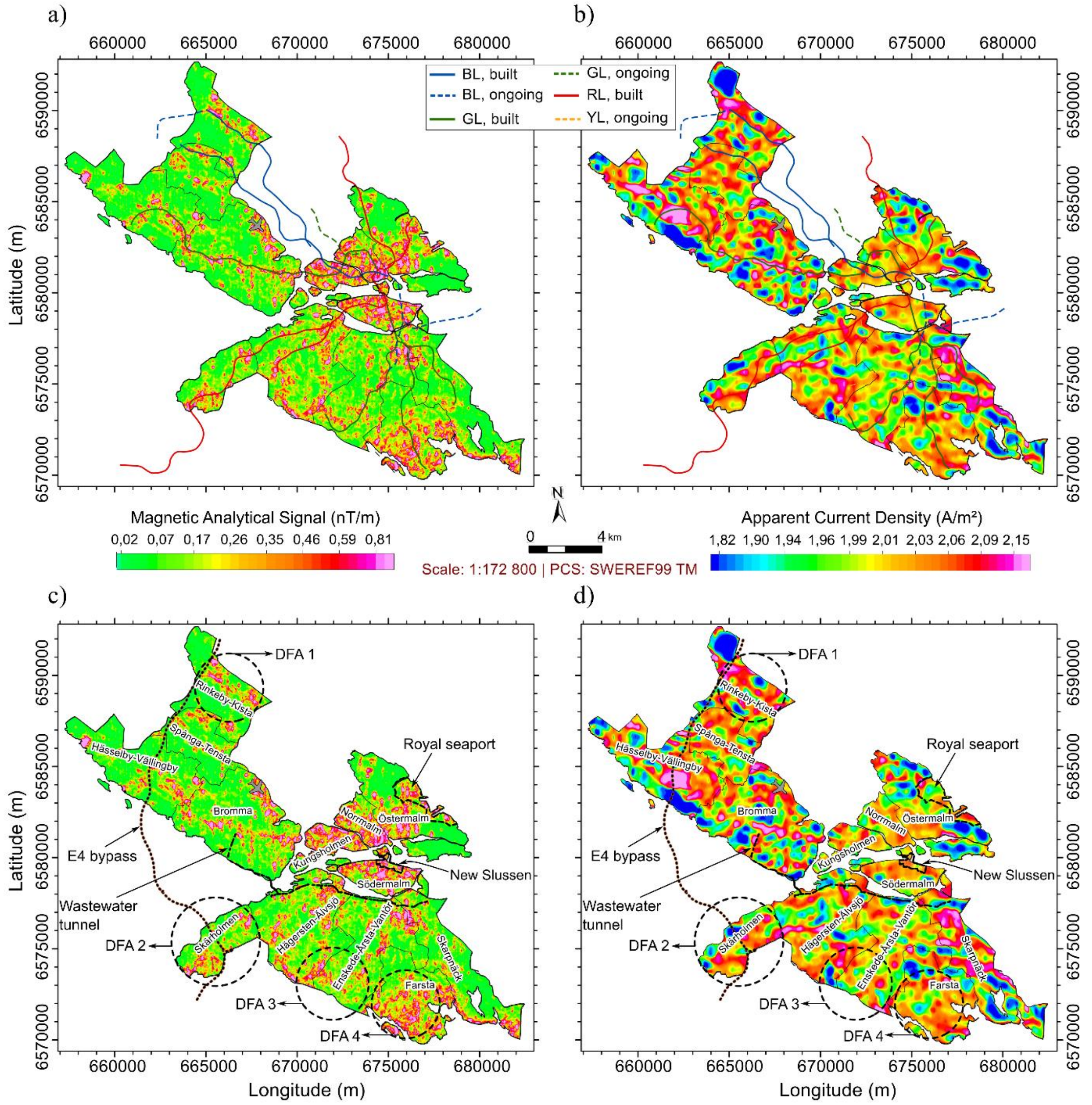

e)

Excerpts From Stockholm City Plan "Vision 2040 – a Stockholm for everyone"

Development focus areas (DFAs)

DFA 1: Kista-Husby-Akalla
→ Planned to be a regional hub.
→ 6000 homes + offices/schools to be built.

DFA 2: Skärholmen-Vårberg
→ Planned to be a regional hub.
→ 4000 homes + 5 recreational facilities to be built.

DFA 3: Hagsätra-Älvsjö
→ Planned to be a regional hub.
→ New homes + 5 schools + 6 recreational facilities to be built.

DFA 4: Fagersjö-Farsta
→ Planned to be a strategic hub for southern suburbs development.
→ New homes + 5 schools + 4 recreational facilities to be built.

Ongoing major developments:

inside the inner city

- Royal Seaport
  → One of the largest urban developments in Europe.
  → 12000 homes + 35000 workplaces + schools to be built.
- New Slussen
  → Major redevelopments in sync with the city's growth and flood management*.
  → A new lock + 2 water channels + a tunnel + bridges + a park + a bus terminal to be built*.

outside the inner city

- Wastewater tunnel → A 14km connection to the eastern treatment facilities.
- E4 bypass → 86% of the 21km European highway's new route is in tunnels**.

*Stockholms Stad, n.d. **Trafikverket, 2024

Figure 2. *Correlation of analytic signal amplitude of the filtered magnetic residual anomaly field and VLF-derived apparent electrical current density with Stockholm's underground metro, (a) and (b), respectively. (c) and (d) are their analyses in relation to the development focus areas (DFAs) of the current Stockholm city plan and a selection of ongoing infrastructural developments summarized in (e). Note how the correlation on both (a) and (b) strongly suggests the metro as the source of the aligned high-magnitude signals and how, by extension, similar signals would indicate the presence of major infrastructures within the DFAs and other development areas in (c) and (d).*

It is then logical that other signatures, particularly on the magnetic analytic signal map, may belong to subsurface structures of anthropogenic origin—e.g., the linear magnetic signature within *Hägersten-Älvsjö*, flanked by the red and ongoing yellow line (Figure 2a). Another such signal, observable on both the magnetic and current maps, correlates with the *Bromma* airport location (denoted with an airplane symbol in Figure 2). Furthermore, the aforementioned magnetic analytic signal density biases within the inner-city area of Stockholm and the *Farsta* district area are also supported by ground truths—e.g., the *Farsta* district area has notable underground structures associated with both the *tunnelbana* and the *Nynäs* railway stations.

However, it is essential to note that the magnetic analytic signal amplitude map has been enhanced for magnetic sources within the average depth of occurrence of the trace target (30 – 35 m depth), whereas the current density map shows the conductivity distribution of structures from the surface to a few tens of meters depth. Thus, some missing signals on the magnetic map, particularly along the *tunnelbana* layout, that are visible on the current map, could be argued to belong to shallower sections of the layout. Conversely, the signals on the latter, which are not observed on the former, can also be attributed to deeper conductors of possible geologic origin. Therefore, the magnetic analytic signal amplitude map forms the primary basis of the analysis for Stockholm's DFAs, with the VLF current density map serving in a secondary capacity.

4.2. Analysis of Stockholm city plan in relation to geophysical images

The current Stockholm city plan ("Vision 2040 – a stockholm for everyone") contains strategic areas, i.e., DFAs (Figure 3a), to be developed into regional hubs that will relieve the stress of the disproportionately higher population density in the inner-city area (*Innerstaden*) compared to the southern (*Söderort*) and western (*Västerort*) areas of Stockholm municipality. The aim is to facilitate a radial population spread into the DFAs in the western and southern areas (see yellow arrows in Figure 3). This is particularly strategic given that the city has the Baltic bay on its eastern border. Notwithstanding, it is imperative to integrate the third (vertical) dimension into the development of these DFAs in order to avoid the current underground situation below the inner area of Stockholm (see the magnetic analytic signal image of its subsurface, Figure 2c). Particularly since there is evidence of existing major infrastructures beneath some of these DFAs as well (e.g., within DFAs 2 and 4). Unlike the surface, the underground space is a non-renewable resource (Bobylev, 2009), which should be tapped sustainably because once transformed, it becomes a permanent feature.

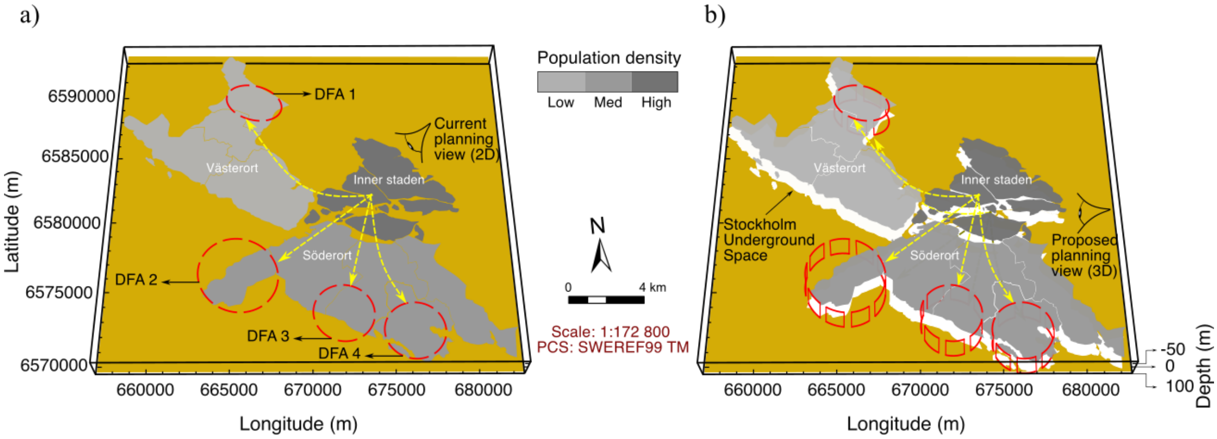

Figure 3. *Comparison between (a) the current model of planning and expansion in Stockholm as evidenced in the city plan and (b) a proposed model based on the geophysical images of Stockholm's underground space.*

Our results do not indicate that vertical expansion below the surface is impossible or should not be undertaken within the inner area of Stockholm. But, we emphasize the need to also have a parallel expansion strategy along the third dimension, as illustrated in Figure 3b. We also propose applying planning expertise and priorities used on the surface to the underground. We recommend the definition of development focus volumes (DFVs) rather than areas (DFAs); this could vary for different counties of a country or even for different cities within a municipality. In Stockholm, for instance, we suggest a volume that reaches a depth of 100 m, based on the average depth of occurrence of infrastructural signatures obtained from magnetic results and publicly available depth information about existing and planned infrastructures. Admittedly, our proposal highlights the limitations of two-dimensional imaging and underscores the need for a detailed three-dimensional model of SUS. Nevertheless, our 2D results show, for the first time, preliminary insights into the state of the space below the cityscape of Stockholm at a municipal scale. This implies that 2D and 3D models of the underground space are not mutually exclusive, especially for underground planning purposes.

5. CONCLUSION

Geophysical imaging based on multiple physical properties provides an effective way to gain insight into the state of the underground space for city planners and designers in situations where such information is not readily available and accessible. Similarly, 2D geophysical images can provide valuable preliminary information when 3D models of the underground space are not available, indicating that 2D imaging and 3D modeling are not mutually exclusive for underground planning. There needs to be good storage of data at the appropriate scale and resolution for realistic imaging and modeling of the urban underground space. In order to forestall the tendency for skewed underground development in favor of the central urban areas of cities, it is necessary to integrate a data-driven underground development plan early-on into the city plan.

6. ACKNOWLEDGMENTS

We express our gratitude for the research grant (grant no: 2021-00106) from the Swedish Research Council Formas, within the National Research Program for Sustainable Spatial Planning (*Nationella forskningsprogrammet för hållbart samhällsbyggande*), which made this study possible. We also thank the Swedish Geological Agency (*Sveriges geologiska undersökning*, SGU) for supplying the geophysical datasets used in this study. We would also like to extend our appreciation to the anonymous reviewers for their valuable feedback.

7. REFERENCES

[1] Admiraal, H., & Cornaro, A. (2016). Why underground space should be included in urban planning policy - And how this will enhance an urban underground future. *Tunnelling and Underground Space Technology*, *55*, 214–220. https://doi.org/10.1016/j.tust.2015.11.013

[2] Bastani, M., Persson, L., Mehta, S., & Malehmir, A. (2015). Boat-towed radio-magnetotellurics - A new technique and case study from the city of Stockholm. *Geophysics*, *80*(6), B193–B202. https://doi.org/10.1190/GEO2014-0527.1

[3] Bastani, M., Wang, S., Malehmir, A., & Mehta, S. (2022). Radio-magnetotelluric and controlled-source magnetotelluric surveys on a frozen lake: Opportunities for urban applications in Nordic countries. *Near Surface Geophysics*, *20*(1), 30–45. https://doi.org/10.1002/nsg.12180

[4] Beamish, D. (1994). Two-dimensional, regularised inversion of VLF data. In *Journal of Applied Geophysics* (Vol. 32).

[5] BeFo. (2018). *Sweden Underground – Rock Engineering and How it Benefits Society* (U. Lindblom, L. Ericsson, T. Winqvist, P. Tengborg, & U. Håkansson, Eds.). BeFo Rock Engineering Research Foundation. https://www.befo.se/publikationer/sweden-underground-rock-engineering-and-how-it-benefits-society/

[6] BeFo. (2020). Nya dimensioner i svensk planering – en utredning om undermarksplanering och geosystemtjänster / New dimensions in Swedish planning- an investigation on subsurface planning and geosystem services. *BeFo Rock Engineering Research Foundation*, *214*. https://www.befo.se/publikationer/nya-dimensioner-i-svensk-planering-en-utredning-om-undermarksplanering-och-geosystemtjanster/

[7] Bobylev, N. (2009). Mainstreaming sustainable development into a city's Master plan: A case of Urban Underground Space use. *Land Use Policy*, *26*(4), 1128–1137. https://doi.org/10.1016/j.landusepol.2009.02.003

[8] Brodic, B., Malehmir, A., Bastani, M., Mehta, S., Juhlin, C., Lundberg, E., & Wang, S. (2017). Multi-component digital-based seismic landstreamer and boat-towed radio-magnetotelluric acquisition systems for improved subsurface characterization in the urban environment. *First Break*, *35*(8), 41–47. https://doi.org/10.3997/1365-2397.35.8.89804

[9] Clarke, R. J. (2000). Planning and mapping of underground space — an overview. *Tunnelling and Underground Space Technology*, *15*(3), 271–286. https://doi.org/10.1016/S0886-7798(00)00056-0

[10] Dahlin, T., & Wisén, R. (2016). Underwater ERT Surveys for Urban Underground Infrastructure Site Investigation in Central Stockholm. *17th Nordic Geotechnical Meeting Challenges in Nordic Geotechnic 25th – 28th of May*. https://www.issmge.org/publications/online-library

[11] Hansen, R. O., Racic, L., & Grauch, V. J. S. (2005). 6. Magnetic Methods in Near-Surface Geophysics. In *Near-Surface Geophysics* (pp. 151–176). Society of Exploration Geophysicists. https://doi.org/doi:10.1190/1.9781560801719.ch6

[12] Jacobsen, B. H. (1987). CASE FOR UPWARD CONTINUATION AS A STANDARD SEPARATION FILTER FOR POTENTIAL-FIELD MAPS. *Geophysics*, *52*(8), 1138–1148. https://doi.org/10.1190/1.1442378

[13] Karous, M., & Hjelt, S. E. (1983). Linear filtering of VLF dip-angle measurements. *Geophysical Prospecting*, *31*(5), 782–794. https://doi.org/https://doi.org/10.1111/j.1365-2478.1983.tb01085.x

[14] Kuchler, M., Craig-Thompson, A., Alofe, E., & Tryggvason, A. (2024). SubCity: Planning for a sustainable subsurface in Stockholm. *Tunnelling and Underground Space Technology*, *144*. https://doi.org/10.1016/j.tust.2023.105545

[15] Nabighian, M. N. (1984). Toward a three-dimensional automatic interpretation of potential field data via generalized Hilbert transforms: fundamental relations. *Geophysics*, *49*(6), 780–786. https://doi.org/10.1190/1.1441706

[16] Nabighian, M. N., Grauch, V. J. S., Hansen, R. O., LaFehr, T. R., Li, Y., Peirce, J. W., Phillips, J. D., & Ruder, M. E. (2005). The historical development of the magnetic method in exploration. *Geophysics*, *70*(6). https://doi.org/10.1190/1.2133784

[17] Naprstek, T., & Smith, R. S. (2019). A new method for interpolating linear features in aeromagnetic data. *Geophysics*, *84*(3), JM15–JM24. https://doi.org/10.1190/geo2018-0156.1

[18] Paal, G. (1965). Ore prospecting based on VLF-radio signals. *Geoexploration*, *3*(3), 139–147. https://doi.org/https://doi.org/10.1016/0016-7142(65)90016-5

[19] Pedersen, L. B., & Oskooi, B. (2004). Airborne VLF Measurements and Variations of Ground Conductivity: A Tutorial. *Surveys in Geophysics*, *25*(2), 151–181. https://doi.org/10.1023/B:GEOP.0000028161.90659.4b

[20] Pedersen, L. B., Persson, L., Bastani, M., & Byström, S. (2009). Airborne VLF measurements and mapping of ground conductivity in Sweden. *Journal of Applied Geophysics*, *67*(3), 250–258. https://doi.org/10.1016/j.jappgeo.2007.11.002

[21] Pedersen, L. B., Qian, W., Dynesius, L., & Zhang, P. (1994). An airborne tensor VLF system. From concept to realization. *Geophysical Prospecting*, *42*(8), 863–883. https://doi.org/10.1111/j.1365-2478.1994.tb00246.x

[22] Rajagopalan, S. (2003). Analytic Signal vs. Reduction to Pole: Solutions for Low Magnetic Latitudes. *ASEG Extended Abstracts*, *2003*(2), 1–4. https://doi.org/10.1071/aseg2003ab136

[23] Roest, W. R., Verhoef, J., & Pilkington, M. (1992). Magnetic interpretation using the 3-D analytic signal. *GEOPHYSICS*, *57*(1), 116–125. https://doi.org/10.1190/1.1443174

[24] Ronczka, M., Wisén, R., & Dahlin, T. (2018). Geophysical pre-investigation for a Stockholm tunnel project: Joint inversion and interpretation of geoelectric and seismic refraction data in an urban environment. *Near Surface Geophysics*, *16*(3), 258–268. https://doi.org/10.3997/1873-0604.2018009

[25] Spector, A., & Grant, F. S. (1970). Statistical models for interpreting aeromagnetic data. *Geophysics*, *35*(2), 293–302. https://doi.org/10.1190/1.1440092

[26] Stockholms stad. (n.d.). *New Slussen*. Retrieved February 14, 2025, from https://vaxer.stockholm/siteassets/stockholm-vaxer/projekt/sodermalm-sdo/sodermalm/slussen/webb/dokument/new_slussen_english.pdf

[27] Stockholms stad. (2018). *Stockholm City Plan*. https://vaxer.stockholm/siteassets/stockholm-vaxer/tema/oversiktsplan-for-stockholm/english_stockholm_city_plan.pdf

[28] Svensson, M. (2016). GeoBIM for optimal use of geotechnical data. *17th Nordic Geotechnical Meeting Challenges in Nordic Geotechnic 25th – 28th of May*. www.trust-geoinfra.se

[29] Tengborg, P., & Sturk, R. (2016). Development of the use of underground space in Sweden. *Tunnelling and Underground Space Technology*, *55*, 339–341. https://doi.org/10.1016/j.tust.2016.01.002

[30] Trafikverket. (2024, January 9). *E4 The Stockholm bypass Project*. https://bransch.trafikverket.se/en/startpage/projects/Road-construction-projects/the-stockholm-bypass/

[31] Volchko, Y., Norrman, J., Ericsson, L. O., Nilsson, K. L., Markstedt, A., Öberg, M., Mossmark, F., Bobylev, N., & Tengborg, P. (2020). Subsurface planning: Towards a common understanding of the subsurface as a multifunctional resource. *Land Use Policy*, *90*. https://doi.org/10.1016/j.landusepol.2019.104316